Nucleic Acids Research, 2004, Vol. 32, No. 11 ***3271–3281***
DOI: 10.1093/nar/gkh646

Interactions of the KWK_6 cationic peptide with short nucleic acid oligomers: demonstration of large Coulombic end effects on binding at 0.1–0.2 M salt

Jeff D. Ballin[1], Irina A. Shkel[1] and M. Thomas Record Jr[1,2,*]

[1]Department of Chemistry and [2]Department of Biochemistry, University of Wisconsin-Madison, Madison, WI 53706, USA

Received April 2, 2004; Revised and Accepted May 19, 2004

ABSTRACT

We quantify Coulombic end effects (CEE) on oligocation–nucleic acid interactions at salt concentrations ([salt]) in the physiological range. Binding constants (K_{obs}; per site, at zero binding density) for the +8-charged C-amidated oligopeptide KWK_6 and short single-stranded DNA oligonucleotides [$dT(pdT)_{|Z_D|}$, where $6 \leqslant |Z_D| \leqslant 22$ is the number of DNA phosphates] were determined as a function of [salt] by fluorescence quenching. For the different DNA oligomers, K_{obs} values are similar at high [salt], but diverge as [salt] decreases because $-S_aK_{obs} \equiv -\partial \ln K_{obs}/\partial \ln a_{\pm}$ increases strongly with $|Z_D|$. For binding of KWK_6 near 0.1 M salt, $-S_aK_{obs}$ is 5.5 ± 0.2 for $dT(pdT)_{22}$, 4.0 ± 0.2 for $dT(pdT)_{10}$ and 2.9 ± 0.2 for $dT(pdT)_6$, as compared with 6.5 ± 0.3 for poly(dT). Similarly, at 0.1 M salt, K_{obs} per site for poly(dT) exceeds K_{obs} for $dT(pdT)_{22}$ by 7-fold, for $dT(pdT)_{10}$ by 50-fold and for $dT(pdT)_6$ by 700-fold. We interpret the reductions in K_{obs} and $|S_aK_{obs}|$ with decreasing $|Z_D|$ as a significant CEE that causes binding to the terminal regions of a nucleic acid to be weaker and less salt dependent than interior binding. We analyze long oligonucleotide-KWK_6 binding data in terms of a trapezoidal model for the local (axial) salt cation concentration on single-stranded DNA to estimate the size of the CEE to be at least seven phosphates on each end at 0.1 M salt.

INTRODUCTION

Oligonucleotides are regularly used as models for polymeric nucleic acids in a wide range of applications, including NMR and crystallographic structural studies, spectroscopic investigations of physical properties, and in the thermodynamic characterization of processes, such as conformational changes and binding interactions. To relate studies of oligonucleotides to those of polymeric nucleic acids, it is necessary to understand how oligomers differ from polymeric nucleic acids. A major source of such differences is the increased contribution of end effects to the behavior of oligonucleotides versus polynucleotides. Two examples are fraying of helices at their ends and end binding modes of ligands to DNA. Another effect, termed the 'Coulombic end effect' (CEE), is important for charge–charge interactions with other species, including proteins, DNA-binding drugs, cationic peptides and salt ions. CEEs are particularly important determinants for the relative stabilities of hairpin and dimer duplex forms of a self-complementary (palindromic) DNA or RNA sequence (1,2).

Many *in vivo* and *in vitro* processes involve oligocationic ligands and/or oligomeric nucleic acids. Are the effects of salt concentration on the thermodynamics of these processes different for oligomeric and polymeric nucleic acids at physiological salt concentration? Most physiological functions of RNA and DNA directly involve binding or folding and are therefore very sensitive to [salt]. Short (oligomeric) RNA structures and their conformational transitions play important roles in RNA function *in vivo*. CEEs should be significant in all processes involving small RNAs, including binding of oligomeric RNA strands to polymeric or oligomeric nucleic acids in the mechanism of gene regulation, silencing and ribozyme catalysis (3). Recently discovered small (22 nt) interfering RNAs (siRNAs) bind to the complementary portion of their target mRNA and tag it for degradation (4). CEEs are predicted to be more important for many polymeric RNA conformations than for DNA because RNA is folded in short secondary and tertiary structures of higher charge density and radius, e.g. tRNA. Short hairpins in such structures are often protein binding sites (5–7). Anomalously, small [salt] dependences of the binding constant have been reported for the binding of proteins to ends of short telomeric DNA (8) and in the binding of cationic (+6) neomycin and other amino glycosides to a short 27 nt RNA hairpin containing the conserved A site in the 16S RNA of the 30S ribosome subunit (9).

Three experimental approaches, and corresponding nonlinear Poisson-Boltzmann (NLPB) and Monte Carlo (MC) calculations, have been used to characterize CEEs. ^{23}Na-NMR on a 20 bp oligonucleotide duplex showed a much smaller relaxation enhancement than for 160 bp double-stranded DNA (dsDNA), consistent with a smaller average local Na^+ concentration at the surface of the 20-mer than for 160 bp DNA, as predicted by NLPB analysis for a cylindrical model of the DNA (10). Effects of oligonucleotide length (number of phosphate charges) on the [salt] dependence of

*To whom correspondence should be addressed. Tel: +1 608 262 5332; Fax: +1 608 262 3453; Email: record@biochem.wisc.edu

the melting temperature T_m of helical nucleic acids have been characterized [(2) and references therein], as have the effect of the length of both an oligocation ligand and the nucleic acid lattice on the [salt] dependence of the binding constant K_{obs} [(11–23) and references therein].

Non-specific binding to polymeric DNA or RNA of a series of oligocationic peptides (13–18), polyamines (19) and cobalt hexammine (20), spanning the range of ligand charge $2 \leqslant |Z_L| \leqslant 10$, have been investigated extensively. In general, binding is largely Coulombic. At high [salt] ($\sim$0.5 M) where binding of these cationic ligands is weak, K_{obs} is small (typically of order unity) and insensitive to oligocation charge ($|Z_L|$). At lower [salt], K_{obs} exhibits a very strong power dependence on [salt] with an exponent ($SK_{obs} \equiv \partial \ln K_{obs}/\partial \ln$[salt] or $S_aK_{obs} \equiv \partial \ln K_{obs}/\partial \ln a_{\pm}$) proportional to the oligocation valence [$SK_{obs} \approx -0.9Z_L$ for binding to polymeric ds nucleic acids and $SK_{obs} \approx -0.7Z_L$ for binding to polymeric single-stranded (ss) nucleic acids]. Thus, as [salt] increases, K_{obs} decreases strongly, approaching unity when extrapolated to 1 M salt. Record *et al*. [(21); see (12) for a review] used an approximate analytic polyelectrolyte theory to analyze SK_{obs} of these experiments and to conclude that salt ion release is the driving force for binding as [salt] is reduced. In this analysis, the authors proposed that ion release from the short oligocation L^{Z+} contributed much less to SK_{obs} than that from polyanionic DNA as a result of a CEE for L^{Z+}. Only recently this proposal has been tested.

Zhang *et al*. (22) compared binding of an oligocation (KWK_6) to a polymeric and oligomeric dT nucleic acids. At 0.1 M salt, binding of the octacationic oligopeptide to a site on polymeric dT was between one and two orders of magnitude stronger than to a site on $dT(pdT)_{10}$, whereas $|S_aK_{obs}|$ was between 50 and 100% larger for poly(dT) than for $dT(pdT)_{10}$. Conversely, K_{obs} for KWK_6 binding to the oligomer versus to the polymer were similar at high salt (>0.4 M Na^+). Analysis of these results led Zhang *et al*. (22) to propose that $\sim$75% of S_aK_{obs} for KWK_6 binding to poly(dT) comes from ion release from the DNA polyelectrolyte, and the remaining 25% from ion release from KWK_6 at 0.1 M salt. Later work (23) demonstrated that affinities and the magnitudes of [salt] dependences of L^{8+} binding to DNA oligomers (with 15, 39 and 69 charges) decreased monotonically as the DNA charge (and length) decreased.

Despite the extant experimental evidence for the significance of CEEs, their importance at experimental salt conditions is not widely recognized and is still debated, as evidenced by the presence of opposing views in Chapters 8 and 11 of a current treatise on nucleic acids (24). This controversy has been summarized recently (2). NLPB calculations and analysis of experimental data for conformational transitions of hairpin (one-strand) and two-stranded DNA oligomers at 0.01–1 M 1:1 salt show that CEEs are an important determinant of the ln[salt] derivative (ST_m) of the transition temperature T_m in this [salt] range, and that the CEE explains the different dependences of ST_m on DNA helix length ($|Z_D|$) for hairpin and two-stranded oligomeric DNA helices (2).

The work presented here quantifies the binding thermodynamics of KWK_6 (L^{8+}) with a series of short dT-oligomers ($6 \leqslant |Z_D| \leqslant 22$) to characterize the transition from polyelectrolyte to oligoelectrolyte behavior. We observe that the per site binding constant K_{obs} and its salt activity ($a_{\pm}$) derivative, S_aK_{obs}, decrease strongly with decreasing number of phosphates per oligonucleotide for lengths $|Z_D| \leqslant 22$. The monotonic dependence of S_aK_{obs} on the number of DNA residues (charges) in oligocation binding processes provides a direct experimental approach to quantify the CEE and demonstrate its importance for ligand–nucleic acid interactions. We develop a qualitative model to describe the salt dependence of oligolysine–DNA association on the basis of predicted trapezoidal (parabolic) axial profile of ion accumulation around the DNA lattice for long (short) oligonucleotides. Analysis of previously published 'long' oligomer binding data in terms of this model indicates that the CEE spans at least 7 nt at each end of a ssDNA at 0.1 M [salt]. In a forthcoming paper, we present a unified analysis of experimental data of the current paper and previous results (22,23) that provides a parametric predictive functional form of the dependence of S_aK_{obs} on DNA charge $|Z_D|$, and quantitatively relate the $|Z_D|$-dependence of S_aK_{obs} to the reduced salt cation accumulation characteristic of the CEE.

MATERIALS AND METHODS

Buffers and reagents

All reagents used were reagent grade, purchased from Sigma Chemical Company (St Louis, MO), Fisher Scientific (Pittsburgh, PA) or Aldrich Chemical Company, Inc. (Milwaukee, WI). All solutions were prepared with 18 MΩ cm^{-1} deionized water. All DNA and peptide solutions used in the titrations described below contained 0.2 mM Na_2EDTA, 5 mM sodium cacodylate, pH 6.0 and enough sodium acetate ('NaOAc') to bring the total salt concentration to the indicated salt concentration.

Peptide. KWK_6-NH_2, (K, L-lysine; W, L-tryptophan), was synthesized using a Perceptive Biosystems Pioneer Peptide Synthesizer with standard Fmoc (fluorenyl-9-methoxycarbonyl) pentafluorophenyl chemistry, purified via high-performance liquid chromatography (HPLC) (see Supplemental Material), and characterized using matrix-assisted laser desorption ionization mass spectroscopy (Biochemistry Instrumentation Facility, Madison, WI). Stock peptide concentrations were determined spectrophotometrically from the tryptophan absorbance at 280 nm in 6 M guanidinium chloride using ε_{280} = 5690 M^{-1} cm^{-1} (25). The extinction coefficients of the KWK_6 dissolved in the buffer described above were then experimentally measured to calculate the inner-filter corrections for the fluorescence titrations ($\varepsilon^{Trp}_{296} = 1700 \pm 100$ $M^{-1}cm^{-1}$, $\varepsilon^{Trp}_{350} < 5$ $M^{-1}cm^{-1}$). The resulting oligopeptide inner-filter correction is small relative to the corresponding correction due to the DNA concentration (see below).

Single-stranded oligo(dT) DNA. The oligonucleotides $dT(pdT)_6$, $dT(pdT)_{11}$, $dT(pdT)_{14}$ and $dT(pdT)_{22}$ were synthesized using an Applied Biosystems 391 PCR-mate automated synthesizer with phosphoramidite chemistry and then purified to >98% homogeneity by using polyacrylamide gel electrophoresis as described elsewhere (26,27). Stock solutions of these oligonucleotides were prepared by dialysis, first against a solution of 10 mM disodium phosphate, pH 6.0, 2 mM Na_2EDTA and 100 mM sodium chloride; followed by three sequential dialyses against 0.5 mM NaOAc at 4°C [SpectraPor dialysis tubing, 1000 MWCO for the $dT(pdT)_{22}$ and $dT(pdT)_{14}$

oligomers, and 100 MWCO for the $dT(pdT)_{11}$ and $dT(pdT)_6$ oligomers]. The DNA nucleotide concentration was determined from the 260 nm absorbance with a Beckman DU-600 spectrophotometer using an extinction coefficient of $\varepsilon_{280} = 8100\ M^{-1}$ (nucleotide) cm^{-1} (28) with a multiplicative conversion factor $|Z_D|/(|Z_D|-1)$ to convert into phosphate concentration, where $|Z_D|$ is the number of phosphates in the oligomer. Extinction coefficients of each DNA were measured for use with the inner-filter corrections [$\varepsilon_{296}^{dT(pdT)_{22}} = 490\ M^{-1}cm^{-1}$, $\varepsilon_{296}^{dT(pdT)_{14}} = 560\ M^{-1}\ cm^{-1}$, $\varepsilon_{296}^{dT(pdT)_{11}} = 470\ M^{-1}\ cm^{-1}$ at 0.075 M NaOAc, $\varepsilon_{296}^{dT(pdT)_{11}} = 600\ M^{-1}\ cm^{-1}$ at 0.105 M NaOAc, $\varepsilon_{296}^{dT(pdT)_6} = 560 M^{-1}cm^{-1}$ at 0.035 M NaOAc and $\varepsilon_{296}^{dT(pdT)_6} = 490\ M^{-1}\ cm^{-1}$ at 0.015 M NaOAc; $\varepsilon_{350}^{DNA} \sim 0\ M^{-1}\ cm^{-1}$ in all cases]. At high DNA concentrations, the inner-filter correction can be as large as 20%.

Fluorescence titrations

Oligopeptide binding to oligo(dT) DNA was monitored by tryptophan fluorescence quenching with an SLM-Amino 8000C spectrofluorometer (Spectronic Instruments, Rochester, NY). The excitation wavelength was 296 nm with a bandpass of 4 nm, and the emission wavelength was 350 nm with a bandpass of 4 nm. These wavelengths were chosen to minimize the inner-filter corrections and DNA absorbance (29). Solutions of the oligopeptides (0.5–5.1 μM) and DNA (1–4 mM DNAP) used in the fluorescence titrations were prepared from freezer stocks and diluted to obtain identical buffer and salt concentrations (pH 6 in 5 mM sodium cacodylate, 0.2 mM Na_2 EDTA and enough NaOAc to bring the total Na^+ concentration to 0.1 M Na^+ [$dT(pdT)_{22}$, $dT(pdT)_{14}$, $dT(pdT)_{11}$], 0.075 M Na^+ [$dT(pdT)_{11}$], 0.035 M Na^+ [$dT(pdT)_6$] or 0.015 M Na^+ [$dT(pdT)_6$].

Use of fluorescence spectroscopy in the determination of binding parameters

The extent of tryptophan fluorescence quenching is defined as

$$Q_{obs} \equiv \frac{|F_{obs} - F_0|}{F_0}, \quad \mathbf{1}$$

where F_{obs} is the observed fluorescence intensity and F_0 is the initial fluorescence intensity of the free ligand (i.e. oligopeptide). All fluorescence intensities were corrected for background fluorescence, dilution, inner-filter contributions and photobleaching effects as described above and elsewhere (22,29).

'Reverse titrations', where the peptide is titrated with DNA, were executed at fixed excess salt concentration to generate binding isotherms. Titrations were typically performed in duplicate or triplicate at 25°C over a range of oligopeptide concentrations (12–17 reverse titrations for each DNA length). At the conclusion of almost all reverse titrations, a 'saltback titration' was performed in which the equilibrated KWK_6–DNA solutions were titrated with a high salt solution (1.00 M NaOAc, 5 mM sodium cacodylate, pH 6, 0.2 mM Na_2EDTA; see Buffers and reagents). The increase in fluorescence (and therefore the decrease in the quenching, Q_{obs}) was monitored as the salt concentration of the solution increased. After all corrections were applied (i.e. background fluorescence, dilution, inner-filter, photobleaching of KWK_6 and photobleaching of the rhodamine reference), >97% of the original fluorescence signal of the free oligopeptide was recovered, indicative of complete reversibility of oligopeptide-DNA complex formation.

Analysis of the oligopeptide–DNA binding isotherms

Determination of equilibrium binding constants from fluorescence quenching. Ligand binding densities (ν) and the concentration of unbound oligopeptide ($[P_F]$) were calculated using ligand binding density function ('LBDF') analysis (29), a model-independent method to show that fluorescence quenching, Q_{obs} (Equation 1), is proportional to the concentration of bound peptide, $[P_B]$, and thus proportional to binding density ($\nu = [P_B]/[D_T]$; see Supplemental Material). $[P_T]$ and $[D_T]$ are the total molar concentrations of KWK_6 and of DNA phosphate, and Q_{max}, the maximum quenching, is attained when all peptide is bound (i.e. when $[P_B]/[P_T] = 1$). To calculate the average binding constant, K_{obs}, of KWK_6 with individual sites on $dT(pdT)_{22}$, $dT(pdT)_{39}$ and $dT(pdT)_{69}$, the dependence of ν on $[P_F]$ was analyzed using a finite lattice model (23,30). This model incorporates anti-cooperativity for large ligand (overlap) effects but neglects CEEs and assumes that all potential binding sites have the same binding constant K_{obs}:

$$\nu = \sum_{j=0}^{J_{max}} \frac{j(K_{obs}[P_F])^j \Omega_j}{|Z_D|\Sigma}, \quad \mathbf{2}$$

where

$$\Sigma = \sum_{j=0}^{J_{max}} (K_{obs}[P_F])^j \Omega_j \quad \mathbf{3}$$

and

$$\Omega_j = \frac{(|Z_D| - (|Z_L| - 1)j)!}{j!(|Z_D| - j|Z_L|)!}. \quad \mathbf{4}$$

In Equations 2–4, Ω_j is the number of arrangements of j ligands (with net charge, $|Z_L|$) on a DNA lattice with $|Z_D|$ phosphates, to a maximum of J_{max} ligands bound. Binding modes in which a peptide extends beyond the end of the DNA lattice are disallowed. The partition function Σ is the sum over all states of binding (30). The Epstein model assumes that there are $||Z_D| - |Z_L|| + 1$ potential binding sites with no overhanging ligands and assumes that K_{obs} is the same for all sites, regardless of site position or the presence of other bound ligands. Because this isotherm neglects differences in binding affinity caused by CEEs near the ends of the lattice, the zero binding density value of K_{obs} is interpreted as an average over all possible sites (see Discussion).

Titration data for the oligomers from $dT(pdT)_6$ to $dT(pdT)_{15}$ were fit to a 1:1 binding model (Equation 5) [mathematically equivalent to the Epstein finite lattice binding model (Equation 2)]:

$$K_{obs} = \frac{|Z_D|\nu}{(||Z_D| - |Z_L|| + 1)(1 - \nu|Z_D|)([P_T] - \nu[D_T])} \quad \mathbf{5}$$

Table 1. Fitted values of the binding constants K_{obs}, salt derivatives (SK_{obs} and S_aK_{obs}), and 1 M intercepts (K_0) for the binding of KWK_6 to dT-mers using LBDF values of Q_{max}

dT-mer	$\|Z_D\|$	Q_{max} (%)	$\log_{10} K_{obs}$ ([Na^+] = 0.105 M)	$-SK_{obs}$[a]	$\log_{10} K_0$[a] (1 M Na^+)	$-S_aK_{obs}$[a]	$\log_{10} K_0$[a] ($a_\pm$ = 1 M)
poly(dT)	169[b]	90 ± 2[c]	6.45 ± .33[d]	6.36 ± .21[c,e]	0.27 ± .15[c,e]	6.54 ± .28[c,e]	−0.70 ± .22[c,e]
dT $(pdT)_{69}$	69[f]	93 ± 2[c]	6.23 ± .16	5.83 ± .11	0.43 ± .12	6.14 ± .14	−0.50 ± .12
dT $(pdT)_{39}$	39[f]	94 ± 2	5.98 ± .10	5.63 ± .10	0.50 ± .07	5.93 ± .12	−0.40 ± .10
dT $(pdT)_{22}$	22	95 ± 1	5.60 ± .04	5.26 ± .22	0.48 ± .17	5.54 ± .16	−0.39 ± .14
dT $(pdT)_{15}$	15[f]	93 ± 2	5.33 ± .07	4.77 ± .27	0.60 ± .23	5.05 ± .22	−0.19 ± .30
dT $(pdT)_{14}$	14	92 ± 1	5.24 ± .05	4.80 ±.33	0.47 ± .28	5.08 ± .38	−0.32 ± .37
dT $(pdT)_{11}$	11	86 ± 1	4.91 ± .03	4.20 ± .31	0.74 ± .26	4.47 ± .36	0.03 ± .35
dT $(pdT)_{10}$	10[b]	90 ± 2	4.72 ± .04	3.75 ± .12	$0.95^{+0.05}_{-0.10}$	3.96 ± .15	0.34 ± .14
dT $(pdT)_6$	6	76 ± 1[g]	3.59 ± .29[d]	2.64 ± .20[h]	1.01 ± .21	2.85 ± .23	0.53 ± .23

Errors are reported with 95% confidence intervals unless otherwise noted (see Materials and Methods for details of Q_{max} and log K_{obs} error determination). Fits to the reverse titration isotherms are shown in Figure 1 and to the salt dependence are in Figure 2A and B.
[a]S_aK_{obs}, SK_{obs} and log K_0 were determined within 0.083 M ≤ $a_\pm$ ≤ 0.19 M (0.105–0.25 M [Na^+]) using the LBDF determined Q_{max}, unless otherwise indicated.
[b]Saltback data (15) reanalyzed within the range considered here.
[c]Values determined at 0.196 M Na^+ because binding is too tight at 0.106 M Na^+ for accurate estimation.
[d]Linearly extrapolated to 0.105 M [Na^+] using Equation 6.
[e]S_aK_{obs}, SK_{obs} and log K_0 were determined within 0.15 M ≤ $a_\pm$ ≤ 0.19 M (0.195–0.25 M [Na^+]).
[f]Saltback data (16) reanalyzed within the range considered here.
[g]Q_{max} value for dT $(pdT)_6$ at 0.035 M Na^+. dT $(pdT)_6$ at 0.015 M Na^+ has $Q_{max} = 80^{+1\%}_{-2\%}$.
[h]Two point determination of S_aK_{obs} and log K_0. log K_{obs} = 4.82 ± 0.04 at 0.035 M Na^+ and log K_{obs} = 5.79 ± 0.06 at 0.015 M Na^+. The reported error in log K_{obs} was calculated via propagation of the log K_{obs} error at these two salt concentrations.

The $(||Z_D| - |Z_L|| + 1)$ term accounts for the statistical degeneracy (number of ways) of binding the shorter oligomer to the longer one, assuming as above that all sites have the same K_{obs}, and that no binding occurs with overhanging ends.

The nonlinear least squares program NONLIN (31) was used to fit Equations 2 and 5 to the fluorescence quenching data obtained from reverse titrations via the LBDF proportionalities (see Supplemental Material). K_{obs} was fit with Q_{max} fixed to the LBDF value (Table 1) and also with Q_{max} floated (Table SII).

Error determination in analysis. For each DNA oligomer, reverse titrations spanning the range of oligopeptide concentrations 0.5–5.1 μM were performed in replicate, as described above. All fitted parameters are reported with 95% confidence intervals unless otherwise indicated. One such exception is in the log K_{obs} values determined directly from reverse titrations. Because of the high number of experimental points involved (typically 60 points or more), fitted errors in log K_{obs} were usually well below 0.5%. To get a better estimation of error in log K_{obs}, fits of the reverse titration data were performed constraining Q_{max} at its upper bound value and its lower bound value. The error in log K_{obs} was then estimated by using the widest possible error range (i.e. using the lower bound log K_{obs} found at the upper Q_{max} fit and the upper bound log K_{obs} value resulting from the lower bound Q_{max} fit). Even using this extreme definition of error in log K_{obs} (reported in Tables 1 and SII), errors in log K_{obs} are in the order of 1%.

We conclude that 95% confidence interval as reported in Tables 1 and SII provide a realistic statement of the uncertainty in $SK_{obs} \equiv \partial \ln K_{obs}/\partial \ln[\text{salt}]$ and $S_aK_{obs} \equiv \partial \ln K_{obs}/\partial \ln a_\pm$. When it was necessary to interpolate or extrapolate values of log K_{obs} using Equation 6, error in S_aK_{obs} (SK_{obs}) and in log K_0 was propagated to estimate the error in log K_{obs}.

Analysis of the salt dependence of log K_{obs} or ΔG^o_{obs}. Over the range of salt concentration examined, the dependence of K_{obs} on salt (mean ionic) activity for each oligonucleotide was well described as a power law dependence with a [salt]-independent exponent. The K_{obs} (Equations 2 and 5) necessary to exhibit the observed ν (via Q_{obs} and Equations S1–S3) at the known peptide and DNA concentrations present in the solution was calculated at each point of the saltback titration. The exponent S_aK_{obs} and the extrapolated ($a_\pm$ = 1 M) reference binding constant K_0 were then determined from the [salt] dependence of K_{obs} (12,21),

$$\log K_{obs} = \log K_0 + (S_aK_{obs}) \log a_\pm. \quad \mathbf{6}$$

The results from the NONLIN least-squares fitting analysis are reported for both fitted values of Q_{max} (Table SII) and from LBDF analysis (Table 1). The S_aK_{obs} data reported here are the linear least squares fits using 95% confidence intervals (see above) of the log K_{obs} versus log $a_\pm$ for data within the salt range of 0.1–0.25 M unless specified otherwise.

The oligopeptide tryptophan fluorescence was independent of [NaOAc] >0.07 M, but decreases monotonically by 20% in the range 0.006–0.07 M NaOAc in the absence of DNA (data not shown). As a result, saltback titrations for $dT(pdT)_6$ are difficult to interpret unambiguously. Therefore, S_aK_{obs} and log K_0 were estimated from Equation 6 using two well-determined values of K_{obs} (from data of 12 reverse titrations) at 0.015 and 0.035 M [Na^+]. K_{obs} at 0.105 M Na^+ for $dT(pdT)_6$ was then obtained from Equation 6 assuming S_aK_{obs} to be independent of salt concentration in this range.

RESULTS

Reverse and saltback titrations to quantify KWK_6–oligo(dT) binding: behavior of Q_{obs} and Q_{max}

Tryptophan fluorescence quenching was monitored during reverse titrations and saltback titrations (see Materials and Methods) to determine the thermodynamics of binding of

the octacationic oligopeptide ligand KWK_6 to ssDNA $dT(pdT)_{|Z_D|}$ with $|Z_D|$ equal to 6,11,14 and 22. Ligand binding density functional analysis ('LBDF') (29) demonstrates that the corrected fluorescence quenching, Q_{obs}, of KWK_6 in the presence of the $dT(pdT)_{|Z_D|}$ oligonucleotides studied here is proportional to the ratio of bound ligand to total ligand ($[P_B]/[P_T]$) (see Supplemental Material Figure S1). This model-independent result, analogous to that obtained previously for poly(dT) (17,22) allows the calculation of ligand binding density directly from the fluorescence quenching data. For $dT(pdT)_{22}$ and $dT(pdT)_{14}$ at 0.105 M Na^+, $dT(pdT)_{11}$ at 0.105 M and 0.075 M Na^+ and $dT(pdT)_6$ at 0.015 and 0.035 M Na^+, values of Q_{max} determined from extrapolation to the condition where all the peptide is bound ($[P_B]/[P_T] = 1$) (Table 1) were the same within error as values of Q_{max} (Table SII in Supplemental Data) found by nonlinear least-squares fitting of reverse titration data to the Epstein or 1:1 binding models as appropriate (cf. Figure 1 and Materials and Methods). As part of this work, previously published data (22,23) for poly(dT), $dT(pdT)_{69}$, $dT(pdT)_{39}$, $dT(pdT)_{15}$ and $dT(pdT)_{10}$ were reanalyzed. The differences between fitted versus LBDF determinations of Q_{max} were within 1 SD for all cases except $dT(pdT)_{15}$ at 0.106 M Na^+.

Q_{max} for KWK_6-oligo(dT) complexes may depend on DNA length for the shorter lengths studied here. Considering only values of Q_{max} determined at 0.105 M Na^+, the quenching upon binding of KWK_6 to $dT(pdT)_{11}$ and $dT(pdT)_{10}$ (86 ± 1 and 90 ± 2%, respectively) are smaller than the average Q_{max} value (93.5 ± 1.3%) observed at higher $|Z_D|$ (Figure S2). Values of Q_{max} for binding of KWK_6 to $dT(pdT)_6$ at 0.015 and 0.035 M NaOAc (80 and 76%, respectively) are smaller than observed for longer dT-oligomers, but a significant [salt] dependence of peptide fluorescence and Q_{max} below 0.1 M salt contributes to this effect.

Reverse titrations of KWK_6 with DNA at constant [salt]

Figure 1 shows reverse titration binding isotherms for KWK_6 binding to $dT(pdT)_{|Z_D|}$ (where $|Z_D| = 22$, 14, 11 and 6) at the indicated salt concentrations. Q_{obs}, directly proportional to the percentage of bound peptide (Equation S1), increases as the total DNA phosphate concentration increases. Eventually, at high [DNA], the fluorescence quenching reaches a plateau, indicating saturation of the peptide. At higher initial peptide concentration, the titration curves as detected by fluorescence quenching shift to higher DNA concentration and sharpen (Figure 1). Complexes with weaker binding affinity (e.g. $dT(pdT)_{11}$–KWK_6 versus $dT(pdT)_{22}$–KWK_6, both at 0.105 M Na^+) require higher [DNA] to achieve saturation at a given KWK_6 concentration. As the binding affinity decreases, isotherms differing in initial oligopeptide concentration coalesce (compare Figure 1A versus C): as K_{obs} decreases, the number of complexes becomes less sensitive to the concentration of DNA present because binding is weaker.

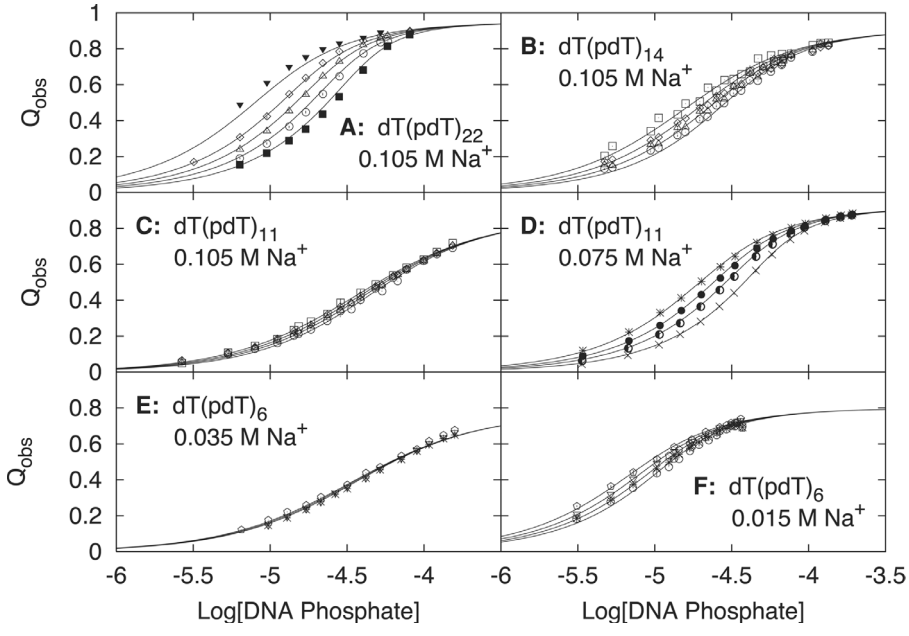

Figure 1. Reverse titrations. Reverse titration binding isotherms obtained at constant ligand concentration by monitoring fluorescence quenching as a function of increasing DNA concentration at pH 6.0 and 25°C. The solid line curves are the theoretical fits to the Epstein model for the specified ligand concentrations using a site size $n = 8$ and the K_{obs} and LBDF Q_{max} values denoted in Table 1. (**A**) KWK_6 binding to $dT(pdT)_{22}$ at 0.105 M Na^+ and initial peptide concentrations of 0.49 μM (black inverted triangles), 1.03 μM (open diamonds), 1.48 μM (open triangles), 2.06 μM (open circles) and 2.94 μM (black squares). (**B**) KWK_6 binding to $dT(pdT)_{14}$ at 0.105 M Na^+ and initial peptide concentrations of 0.59 μM (open squares), 1.03 μM (open diamonds), 1.48 μM (open triangles) and 2.06 μM (open circles). (**C**) KWK_6 binding to $dT(pdT)_{11}$ at 0.105 M Na^+ and initial peptide concentrations of 0.59 μM (open squares), 1.03 μM (open diamonds), 1.48 μM (open triangles) and 2.06 μM (open circles). (**D**) KWK_6 binding to $dT(pdT)_{11}$ at 0.075 M Na^+ and initial peptide concentrations of 1.73 μM (asterisks), 2.54 μM (black circles), 3.40 μM (half moons) and 5.08 μM (crosses). (**E**) KWK_6 binding to $dT(pdT)_6$ at 0.035 M Na^+ and initial peptide concentrations of 0.97 μM (open pentagons), 1.29 μM (open inverted triangles) and 1.62 μM (asterisks). (**F**) KWK_6 binding to $dT(pdT)_6$ at 0.015 M Na^+ and initial peptide concentrations of 0.98 μM (open pentagons), 1.30 μM (open inverted triangles), 1.60 μM (asterisks) and 1.94 μM (open circles).

The curves represent global nonlinear fits (Table 1) to the non-cooperative Epstein binding model (Equation 2) for $dT(pdT)_{22}$ or to the mathematically equivalent 1:1 binding model (Equation 5) for the shorter oligomers. LBDF Q_{max} values (Table 1) were used to calculate the average binding density (Equations 2, 5 and S2) in these determinations. In all cases, especially for the shorter oligos ($|Z_D| \leqslant 22$), global fits using the Epstein isotherm and the 1:1 binding model describe the reverse titration data extremely well. Values of the per site binding constant K_{obs} at zero binding density obtained from this fits are an average for all $|Z_D|-7$ sites on the DNA oligomer. As $|Z_D|$ increases, the per site K_{obs} at fixed [salt] increases dramatically (Table 1). K_{obs} at 0.105 M NaOAc is 5-fold larger for KWK_6 binding to $|Z_D| = 22$ than to $|Z_D| = 11$ and 20-fold larger for binding to $|Z_D| = 11$ relative to the extrapolated value of K_{obs} of $|Z_D| = 6$ at this salt concentration. This decrease in K_{obs} with decreasing $|Z_D|$ indicates a strong CEE in L^{8+} binding at 0.1 M salt (see Discussion).

[Salt] dependence of KWK_6–DNA binding

The complexes formed in each reverse titration shown in Figure 1 were titrated with buffered 1 M NaOAc (see Materials and methods and Supplementary Material). Complexes dissociated with increasing [salt] as indicated by a monotonic decrease in the fluorescence quenching. At sufficiently high [salt], Q_{obs} is reduced to <2% for all oligo(dT) lengths studied, indicating that complex formation is fully reversible and that binding is highly [salt] dependent, consistent with previous observations (17,22,23,29).

K_{obs} is determined from Q_{obs} as a function of [salt] via the Epstein finite lattice isotherm or the 1:1 binding model and LBDF-derived binding densities (Figures 1 and S3). Figures 2 and S4 show the variation of $\log K_{obs}$ with salt activity and [salt]. Values of $|S_aK_{obs}|$, evaluated over a specified [salt] range (Table 1), decrease from the polymer limit as DNA length decreases. In Figure 3, as $|Z_D|$ decreases, $|S_aK_{obs}|$ (plotted as a fraction of the experimental value of $|S_aK_{obs}|$ for polymeric dT) exhibits a hyperbolic dependence on $|Z_D|$. For large $|Z_D|$ ($|Z_D| \geqslant 39$), $|S_aK_{obs}|$ decreases gradually with decreasing $|Z_D|$: we refer to such oligomers as long (see Discussion). The decrease becomes much more pronounced for the shorter DNA lengths studied here ($|Z_D| \leqslant 22$): we refer to such oligomers as short (see Discussion). These same data, when plotted versus reciprocal number of DNA charges, is approximately linear over the full range studied, and extrapolation to infinite DNA length ($|Z_D| \rightarrow \infty$) provides an independent determination of the S_aK_{obs} for poly(dT) (-6.4 ± 0.1) (cf. Figure 3, inset).

For each $dT(pdT)_{|Z_D|}$ oligomer, $|S_aK_{obs}|$ decreases with increasing [salt] above ~0.3 M Na^+. At higher [salt], values of K_{obs} for the binding of KWK_6 to DNA oligomers with different $|Z_D|$ appear to converge into a common curve (independent of Z_D). Nevertheless, the data are well fit in the range of 0.1–0.25 M salt by a constant S_aK_{obs}, and thus values for S_aK_{obs} and the extrapolated $\log K_{obs}$ at $a_\pm = 1$ M ($\log K_0$) were determined using linear least squares analysis. Figure 2A suggests that the linear extrapolation of the low [salt] range $\log K_{obs}$ versus log[salt] data to higher [Na^+] may intersect at a common point within the uncertainty of the fit. If the data are

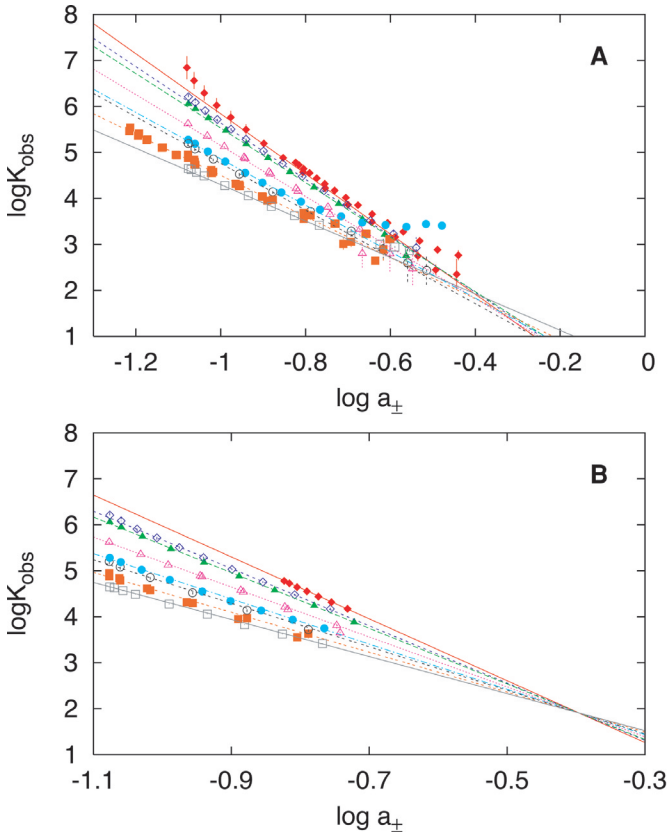

Figure 2. S_aK_{obs} analysis. Log-log plot of K_{obs} versus mean ionic activity ($a_\pm$) of NaOAc for KWK_6 binding to poly(dT) (red diamonds), $dT(pdT)_{69}$ (open purple diamonds), $dT(pdT)_{39}$ (green triangles), $dT(pdT)_{22}$ (open pink triangles), $dT(pdT)_{15}$ (light blue circles), $dT(pdT)_{14}$ (open black circles), $dT(pdT)_{11}$ (orange squares) and $dT(pdT)_{10}$ (open gray squares). The lines in (**A**) represent the least squares linear fits of all data between 0.1 and 0.25 M NaOAc using the parameters summarized in Table 1. The solid and dashed lines in (**B**) represent the global fits of the indicated data to Equation 6, constrained to intersect at a single extrapolated value (see Table SIII in the Supplementary Material).

globally constrained to have a common intersection point (Figure 2B), the resulting S_aK_{obs} values (Table SIII) are within error of those analogously determined from fitting individual KWK_6-oligomers (Table 1). Allowing for the possibility of two intersection points, e.g. one for longer length DNA [poly(dT)–$dT(pdT)_{39}$] and another for shorter lengths [$dT(pdT)_{22}$–$dT(pdT)_{10}$], does not significantly improve the fit. The intersection on Figure 2B occurs at $a_\pm = 0.40 \pm 0.04$ M Na^+ ([Na^+] = 0.53 M) with a $\log K_{obs}$ of 1.91 ± 0.20. This point represents an extrapolated reference state describing the DNA-length independent contribution to the binding of KWK_6 to a ssdT-oligomer. Interestingly, the analogous fitting of $\log K_{obs}$ versus log[Na^+] (Figure S4) results in the same reference point ($\log K_{ref} = 1.89 \pm 0.20$, $[Na^+]_{ref} = 0.55 \pm 0.07$ M), although analysis on the mean activity scale exhibits a better statistical fit on the basis of the variance. Studies of binding of a series of oligocationic ligands (13,17) to polymeric nucleic acids also yield a common intersection point between 0.5 and 1 M salt.

Values of S_aK_{obs} for poly(dT), $dT(pdT)_{69}$, $dT(pdT)_{39}$, $dT(pdT)_{15}$ and $dT(pdT)_{10}$ reported in Table 1 differ in some

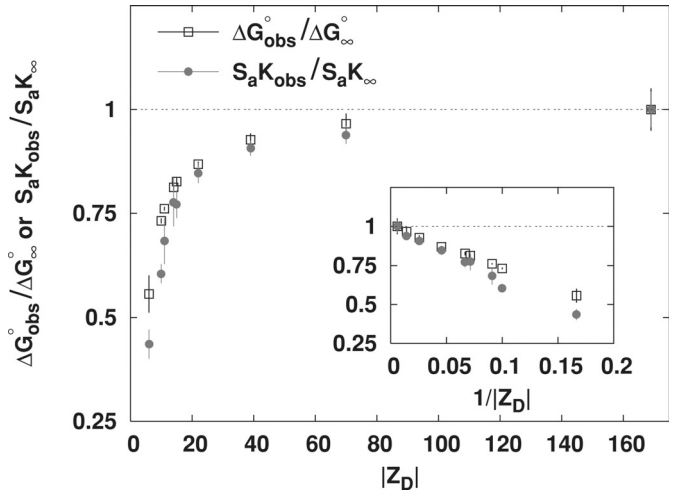

Figure 3. Dependence of ΔG^{o}_{obs} (0.1 M Na^+) and S_aK_{obs} on number of DNA charges $|Z_D|$. Values of ΔG^{o}_{obs} at 0.1 M Na^+ (open squares) and S_aK_{obs} (circles), normalized by the corresponding quantities for binding of KWK_6 to poly(dT), are plotted against the number of DNA charges $|Z_D|$. Reanalysis of data published previously (22,23) and current work are detailed in Table 1. S_aK_{obs} was determined as the slope of Equation 6 fit in the log$a_{\pm}$ range of −1.1 to −0.72 (∼0.1–0.25 M [Na^+]; cf. Figure 2B). All ΔG^{o}_{obs} values were determined from reverse titrations with the exception of $dT(pdT)_6$, for which ΔG^{o}_{obs} was obtained by linear extrapolation of the log K_{obs} vesus log$a_{\pm}$ to 0.105 M Na^+ (Equation 6). The inset plots the same data versus $1/|Z_D|$.

cases from values published previously (22,23) because a smaller salt range was considered (0.1–0.25 versus 0.1–0.3 M Na^+) for consistency with other oligo(dT) lengths investigated in this study.

Dependence of ΔG^{o}_{obs} on $|Z_D|$

Values of $\Delta G^{o}_{obs} = -RT \ln K_{obs}$ at 0.105 M Na^+ and 25°C, either determined directly by reverse titration (Figure 1) or via Equation 6 using S_aK_{obs} and log K_0, were normalized by the corresponding value for poly(dT) and plotted as a function of DNA charge in Figure 3. The general features in the plot of $\Delta G^{o}_{obs}/\Delta G^{o}_{\infty}$ versus $|Z_D|$ at 0.105 M Na^+ are similar to those seen for S_aK_{obs}/S_aK_{∞} versus $|Z_D|$: ΔG^{o}_{obs} increases strongly with increasing $|Z_D|$ when $|Z_D| \leqslant 15$, but is only weakly dependent on DNA length for oligonucleotide lengths $|Z_D| \geqslant 39$ phosphates. As $|Z_D|$ increases above $|Z_D| = 22$, ΔG^{o}_{obs} (expressed per site on the DNA lattice) gradually approaches ΔG^{o}_{∞} for poly(dT). Above $|Z_D| = 39$, both ΔG^{o}_{obs} (0.1 M) and S_aK_{obs} are within uncertainty of the values for poly(dT). Deviations of ΔG^{o}_{obs} from the poly(dT) limit are approximately linear in $1/|Z_D|$, as are deviations of S_aK_{obs} from the poly(dT) limit (Figure 3, inset).

The range of $|Z_D|$ where ΔG^{o}_{obs} is strongly dependent on $|Z_D|$ is the same as that where S_aK_{obs} is strongly dependent on $|Z_D|$. Thus, short oligomers defined above in terms of strong effect of length ($|Z_D|$) on K_{obs} exhibit strong effect of length on the salt dependence S_aK_{obs} as well. In Discussion, we relate this behavior to the presence (for long oligomers) or absence (for short oligomers) of a polyion-like interior region in the surface axial counterion distribution.

DISCUSSION

The Coulombic end effect

The Coulombic interactions of nucleic acids with salt ions in solution create strong radial gradients of ion density, accumulating salt cations and excluding salt anions in the vicinity of the nucleic acid. The binding of an oligocationic ligand changes these gradients and gives rise to the remarkably large dependence of the equilibrium constant on [salt]. Binding constants of oligiocationic ligands to polymeric nucleic acids exhibit power dependences on [salt] (cf. Equation 6) with exponents SK_{obs}, which are proportional to the ligand charge (11,12). For example, the K_{obs} for binding L^{8+} to polymeric ss- or ds-DNA is predicted to change by 5–7 orders of magnitude for each decade change in [salt]. A general, model-independent thermodynamic analysis (12,32) connects the [salt] derivative SK_{obs} of a charged biopolymer process to the change in salt ion preferential interaction coefficients

$$S_aK_{obs} = \Delta(|Z| + 2\Gamma), \quad 7$$

where $\Delta\Gamma$ is the change in preferential interaction coefficients describing interactions of salt ions with product and with reactants, and $\Delta|Z| = |Z_{LD}| - |Z_D| - |Z_L|$, where Z_{LD}, Z_D, and Z_L are charges of ligand-DNA complex (LD), DNA (D) and ligand (L), respectively (12,32). The difference $\Delta\Gamma$ describes the redistribution of the salt ions caused by the local neutralization of peptide and DNA charges upon complexation. This redistribution is the molecular origin of the salt ion release upon binding (12,33).

The Coulombic interactions of salt ions and ligands with phosphates in the terminal regions of a nucleic acid are very different than those involving interior phosphates of a long nucleic acid (1,2,12,22,23,33–35). Binding of a cationic ligand to the terminal regions is predicted (33) and deduced from experiment [Figure 3 and (22,23)] to be less [salt] dependent and weaker at low [salt] than interior binding. We call these differences CEEs. The CEE should be especially important when comparing effects of [salt] on processes involving short nucleic acid oligomers (lacking a polyelectrolyte-like interior region, as discussed below) with those of the corresponding polyion. CEEs cause the strong dependencies on DNA chain length ($|Z_D|$) of SK_{obs} for oligocation binding reported here [see also (22,23)]. Computational (both GCMC and NLPB) analyses (22,23,33) show that the strong reduction in S_aK_{obs} with decreasing $|Z_D|$ for short oligos is a consequence of the CEE, arising from the reduced cation accumulation at the ends of all nucleic acids, and in the interior of sufficiently short nucleic acids.

CEE: axial dependence of surface concentrations of salt cations, anions; consequences for average K_{obs}, SK_{obs}

Monte Carlo simulations (33,36) and NLPB calculations [(2,35) and Figure S6] which model DNA as a primitive cylinder show that the salt cation concentration in the vicinity of the DNA surface is very high and uniform in the interior, but falls off strongly in the terminal regions of sufficiently long oligomers, resulting in a 'trapezoidal' axial profile of the local salt cation concentration. For these long oligomers, as $|Z_D|$ increases, the length of the interior region increases, but the lengths of the terminal regions remain the same. The number

of DNA phosphates charges (N_e) in each terminal region of a long oligomer does not change as $|Z_D|$ increases. Short oligomers (e.g., less than 20 phosphates for ssDNA at 0.1 M salt [see Figure S6 and (36)] exhibit a 'parabolic' axial cation concentration distribution where the surface cation concentration in the interior region of DNA is predicted to increase with increasing number of phosphates (charges). Above ~20 phosphates, a polyion-like interior is predicted.

In complexation, the salt ion concentration gradients in the vicinity of the DNA and the peptide are reduced, corresponding to a net salt ion release that drives complexation as the bulk salt concentration is reduced (33). If the DNA is long enough to have polyion-like interior region of sufficient length to bind the ligand, binding to those interior sites will exhibit the same K_{obs} and SK_{obs} as binding to the interior of a polyanionic DNA. The N_e terminal sites at each end of this long DNA include one or more phosphates in the terminal region of ion accumulation. As a consequence, binding to such sites exhibits less than the polyion level of ion release, and therefore is characterized by a weaker K_{obs} and a smaller contribution to SK_{obs}. The closer the terminal site is to the DNA terminus, the weaker the binding. $|Z_L| + 2N_e$ (two full terminal regions of N_e phosphates each, and an interior of $|Z_L|$ phosphates) is the minimal DNA chain length necessary to have at least one site that binds a Z_L-charged ligand with polyion values of K_{obs} and SK_{obs}. DNA oligomers with less than $|Z_L| + 2N_e$ charges lack any such interior polyion-like site, and thus complexation at all sites is characterized by smaller K_{obs} and $|SK_{obs}|$. Because most of the binding of ligands to long oligos is to the polyion-like sites in the interior (and not to the weaker sites in the terminal regions), DNA oligomers with $|Z_D| > |Z_L| + 2N_e$ exhibit only gradual reductions in overall (average) K_{obs} and $|SK_{obs}|$ as $|Z_D|$ decreases. Oligomers shorter than $|Z_L| + 2N_e$ show strong reductions in K_{obs} and $|SK_{obs}|$ with decreasing $|Z_D|$ because in this length range binding to interior sites is weaker and releases fewer salt ions. For our experiments, the transformation from a strong to a weak dependence of K_{obs} and S_aK_{obs} on $|Z_D|$ (Figure 3) occurs between dT(pdT)$_{39}$ and dT(pdT)$_{22}$; i.e. $22 < |Z_L| + 2N_e < 39$ (for both $\log K_{obs}$ and SK_{obs}), suggesting that N_e is in the range of 7–15 since $|Z_L| = 8$ for KWK_6. The analysis in the following section tests this picture.

Implications for axial dependence of L^{Z^+} binding constant K_i and for length ($|Z_D|$) dependence of average K_{obs}, SK_{obs} at zero binding density

The trapezoidal model for the binding of L^{Z+} to a long oligonucleotide ($|Z_D| \geqslant 39$) partitions binding into two regimes: one consisting of the interior sites (those exhibiting polyelectrolyte binding affinity and forming the plateau region of the trapezoid), and the other made up of the two terminal regions of N_e binding sites each, where binding affinity decreases with increasing proximity to the termini of the DNA. If a DNA oligomer is long enough ($|Z_D| \geqslant |Z_L| + 2N_e$), the interior sites demonstrate polymeric binding behavior, K_∞,

$$K_\infty = \frac{[PD_\infty]}{[P_F][D]}, \quad \mathbf{8}$$

where PD_∞ is a complex of the peptide P at an interior DNA site and [D] and [P_F] are concentrations of free DNA and KWK_6 molecules. The trapezoidal model holds that all interior sites (as compared to the terminal sites described below) are identical and thus bind peptides with the same affinity, K_∞.

Binding of a peptide to a DNA near a terminus forms a complex PD_i, where $i = 1$ for a complex in which the peptide binds at the terminus of the nucleic acid, $i = 2$ for a complex starting at the second site from the end, and so on. In the low-binding density limit, the binding constant K_i for forming PD_i is

$$K_i = \frac{[PD_i]}{[P_F][D]}, \quad \mathbf{9}$$

where K_i is always less than K_∞ for all sites $i \leqslant N_e$ away from a DNA terminus.

The zero binding density binding constants, K_{obs}, obtained from Epstein or 1:1 isotherms, are extrapolated values representing per site averages over all these potential oligocation binding sites. Neglecting binding modes where the peptide overhangs the nucleic acid, there are $|Z_D| - |Z_L| + 1 = |Z_D| - 7$ sites for KWK_6 ($Z_L = 8$) on the dT-oligomers with $|Z_D| \geqslant 8$ phosphates. In the low-binding density (no multiple binding) limit, the relationship between K_{obs} and K_i is obtained from the McGhee-von Hippel definition of K_{obs} (37):

$$K_{obs} = \frac{\sum[\text{complexes}]}{[\text{free peptide}][\text{free DNA sites}]} = \frac{\sum_{i=1}^{\|Z_D|-|Z_L\|+1} K_i}{\|Z_D|-|Z_L\| + 1}, \quad \mathbf{10}$$

where the concentration of free lattice sites is ($|Z_D| - |Z_L| + 1$) [D] because there are ($|Z_D| - |Z_L| + 1$) sites on each DNA strand. The total concentration of complexes is a sum of all complexes, $[\text{complexes}] = (|Z_D|-|Z_L| + 1 - 2N_e)[PD_\infty] + 2\sum_{i=1}^{i=N_e}[PD_i]$. Therefore, for long oligomers, K_{obs} is the weighted average of the polymeric interior sites and the terminal sites:

$$K_{obs} = \frac{\overbrace{\left[(\|Z_D| - |Z_L\| + 1 - 2N_e)K_\infty\right]}^{\text{interior sites}} + \overbrace{\left(2\sum_{i=1}^{N_e} K_i\right)}^{\text{terminal sites}}}{\|Z_D|-|Z_L\| + 1}. \quad \mathbf{11}$$

For oligomeric DNA strands long enough to exhibit an interior region with polymeric (polyelectrolyte) properties, ΣK_i is expected to be independent of $|Z_D|$. ΣK_i represents the sum of the binding constants for all binding sites in a single terminal region. Since the ΣK_i contribution to K_{obs} does not change for long oligomers, the long oligomer data can be easily analyzed as presented in the next section. However, such simplification is not possible for short oligomers because ΣK_i depends not only on the binding site i, but also on the DNA oligomer length $|Z_D|$. In a forthcoming paper, we develop a quantitative treatment that predicts K_i for both long and short DNA lengths. In the current analysis, we restrict consideration to long oligos only.

Behavior of K_{obs}, S_aK_{obs} as functions of $|Z_D|$, [salt]

In the binding of the KWK_6 octacation (L^{8+}) to a dT oligoanion with $|Z_D|$ negative charges, both the per site K_{obs} and $|S_aK_{obs}|$ decrease strongly with decreasing $|Z_D|$, especially below $|Z_D| = 39$. Reduction of $|Z_D|$ from 39 to 10 charges

causes a 50% reduction in $|S_aK_{obs}|$. The behavior of $\log K_{obs}$ at 0.1 M salt mirrors that of S_aK_{obs} as seen in Figure 3 because the linearly extrapolated $\log K_0$ intercepts are close to zero (Table 1). The small extrapolated K_{obs} seen at high salt concentrations is typical of non-specific interactions of oligocations (polyamines, oligolysines, etc.) with nucleic acid polyanions and indicates that salt ion release, quantified by S_aK_{obs}, represents the dominant driving force for complexation at low to moderate salt concentrations (11,12,14–17,21–23). Since K_{obs} is approximately independent of $|Z_D|$ at high [salt], the variation in K_{obs} with $|Z_D|$ at any lower [salt] is primarily a result of the variation of S_aK_{obs} with $|Z_D|$. Therefore, if we understand why S_aK_{obs} depends on DNA length, we can also understand the variation in K_{obs}.

If we assume that $K_\infty = K_{obs}$ for $|Z_D| = 169$, Equation 11 predicts that the average number of sites at one end of a 39mer ($|Z_D| = 39$) is $N_e = (7 \pm 3) + \Sigma K_i/K_\infty$ at 0.2 M Na^+ or $N_e = (11 \pm 4) + \Sigma K_i/K_\infty$ at 0.1 M Na^+. Since $\Sigma K_i/K_\infty$ must be a positive number, N_e must exceed 7 phosphates (~25 Å) at 0.1 M salt.

At intermediate lengths ($|Z_D| \approx |Z_L| + 2N_e$), binding of the oligocation to a significant portion of the DNA sites is predicted to be weaker than polymeric binding. Therefore, as the total number of sites decreases, the contribution of end sites increasingly dominates the average per site K_{obs}, as seen in Figure 3 and reported in Table 1. Even if the $\Sigma K_i/K_\infty$ term is neglected at 0.2 M Na^+, the first oligonucleotide long enough to have a single polymeric site is $|Z_D| = (|Z_L| + 2N_e) \approx 22 \pm 6$ for KWK_6 binding to ssDNA. Given these results, $dT(pdT)_{22}$ ($|Z_D| = 22$) is near the threshold of exhibiting polymeric binding. This is consistent with the results shown in Figure 3, where $dT(pdT)_{22}$ is at the transition between long and short oligomer binding behavior. Conversely, if there were no CEEs under these conditions, the $\Sigma K_i/K_\infty$ term would equal N_e because there would be N_e polymeric sites for N_e phosphates. In this case, $K_{obs} = K_\infty$ regardless of DNA length, in contrast to what is seen in Figure 3.

The number of end phosphates in the above analysis is greater than that estimated previously (23) because of the use of a trapezoidal (multistate) model instead of a two-state model for binding sites. The two-state model effectively divides each terminal region into half, treating the outward half as a uniform end region and inward half as part of the polymeric interior. As such, N_E is expected to be about half of the total number of end sites predicted by the trapezoidal model. Furthermore, once oligos are in the parabolic regime, as DNA charge decreases, the amount of salt cation accumulation within the oligo interior decreases, and thus the binding affinity decreases. As a result, the binding of a KWK_6 to $dT(pdT)_{10}$ will be weaker than a KWK_6 binding inside the terminal region of a long oligomer. Our previous phenomenological analysis (23) underestimated the ion release associated with end binding by assuming that it is represented by the S_aK_{obs} of KWK_6-$dT(pdT)_{10}$, therefore underestimating N_E as well, and is superseded by the current analysis.

Asymmetric contributions of L^{8+} and poly(dT) to S_aK_{obs} of binding at 0.1 M salt

The data of Table 1 allow us to refine our previous estimate (22) of the contribution of ion release from L^{8+} and from poly(dT) to S_aK_{obs}. Although binding of L^{8+} to $dT(pdT)_8$ was not investigated, the S_aK_{obs} for binding L^{8+} to $dT(pdT)_8$ should be well approximated by the average values of S_aK_{obs} for binding L^{8+} to $dT(pdT)_6$ and $dT(pdT)_{10}$: $S_aK_{obs} = -3.4 \pm 0.3$. Ion release from the oligopeptide and the oligonucleotide should contribute approximately equally to this S_aK_{obs}; this contribution (−1.7) should be the same for L^{8+} binding to all larger dT-oligomers. Hence, for binding L^{8+} to poly(dT) where $S_aK_{obs} = -6.5 \pm 0.3$ at 0.1 M salt, ion release from L^{8+} contributes ~25% and ion release from poly(dT) contributes ~75% of S_aK_{obs}. This asymmetry is a consequence of the CEE; L^{8+} is a short oligoelectrolyte and poly(dT) is a polyelectrolyte. CEEs are very important for L^{8+} but not for poly(dT) in this binding interaction.

Consequences of the CEE for multiple binding

Multiple-ligand binding events are important in the analysis of non-specific binding. In the data presented here, $dT(pdT)_{22}$ and longer lengths are in the multiple binding regime. Models frequently used for analyzing experimental titration data assume a uniform binding constant along DNA [e.g. the Epstein (30) and McGhee–von Hippel (37) models] and introduce cooperative or non-cooperative corrections for multiple binding via the cooperativity factor (37). This approach fits the data well, but does not address the important question of how much the binding differs between the center and the end of an oligomer. The binding affinity presumably depends not only on its position on the DNA but also on the number and positions of other bound ligands.

Binding of the first KWK_6 to a sufficiently short ssDNA (15–39 phosphates) is expected to reduce the effective K_{obs} for subsequent binding by requiring one or both ligands to bind at sites away from higher affinity interior sites and/or by reducing the overall amount of ion release for the next ligand. For example, binding of KWK_6 to the center site of a 39mer DNA strand should be as strong as binding to a site on poly(dT). In the 1:1 central complex on the 39mer, two 16mer regions remain on either side, which are too short to exhibit a trapezoidal ion distribution. Therefore, any second binding event must be weaker per site than the first. This is consistent with GCMC calculations (33), which predicted that ligand binding (modeled as the neutralization of $|Z_L|$ charges in the center of a B-DNA strand) resulted in net reduction of the local counterion concentrations on either side of the site of complexation. Analysis of $dT(pdT)_{39}$ data allowing for varying microscopic binding constants is not straightforward as a result of the combinatorics of multiple binding modes; however, KWK_6-$dT(pdT)_{22}$ binding does not suffer this complication.

If we allow there to be two different average binding constants ($K_{obs,1}$ and $K_{obs,2}$) in the analysis of the $dT(pdT)_{22}$ reverse titration data (Figure 4), the binding density is defined as

$$\nu = \frac{1}{|Z_D|}\frac{\Omega_1 K_{obs,1}[P_F] + 2\Omega_2 K_{obs,1}K_{obs,2}[P_F]^2}{\left(1 + \Omega_1 K_{obs,1}[P_F] + \Omega_2 K_{obs,1}K_{obs,2}[P_F]^2\right)} \quad \mathbf{12}$$

where Ω_j is as defined in Equation 4, the resulting fit is significantly better than that of the Epstein model where only one global K_{obs} is used. An F_χ-test (38) indicates that the improved quality of fit cannot be simply explained by the increase in the

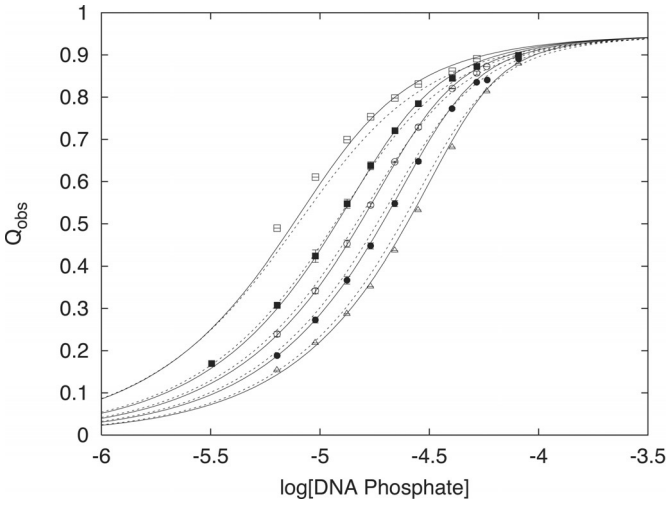

Figure 4. Comparison of fitting models for KWK_6 binding to dT(pdT) $_{22}$ at 0.105 M Na^+ with $Z_L = 8$, $|Z_D| = 22$, and $Q_{max} = 0.95$. Symbols are as defined in Figure 1. The dashed line represents the global fit to the Epstein model (Equation 2) with $\log K_{obs} = 5.605 \pm 0.01$. The solid line is the improved global fit to an Epstein model where two ligands can bind (Equation 12) with different affinities $K_{obs,1}$ and $K_{obs,2}$: $\log K_{obs,1} = 5.734 \pm 0.01$ and $\log K_{obs,2} = 5.434 \pm 0.02$. The F_χ-value (38), which tests the statistical significance of an increase in the number of fitting parameters, confirms that the use of two different binding constants describes KWK_6-dT(dT)$_{22}$ binding better (at a 95% confidence level) than the Epstein model with only one binding constant.

number of fitting parameters. At 0.1 M salt, $K_{obs,2}$ is a factor of two smaller than $K_{obs,1}$, and the two binding constants bracket the Epstein model K_{obs} (cf. Figure 4). The weaker $K_{obs,2}$ suggests that the first ligand binding event adversely affects the binding of a second KWK_6 oligopeptide. The significant difference between Epstein K_{obs} and $K_{obs,1}$ suggests that application of Epstein model to treat L^{Z+}-DNA binding may introduce error in K_{obs} and for more accurate treatments of experimental data one needs a binding isotherm that accounts for CEEs.

CONCLUSIONS

The current study uses a cationic oligopeptide (L^{8+}) as a probe for the thermodynamics of CEEs on oligocation–nucleic acid interactions for a series of relatively short oligonucleotides. The CEE causes $|SK_{obs}|$ and K_{obs} of L^{8+} binding at moderate to low salt concentration ($\leq$0.3 M) to decrease strongly for short oligonucleotides ($|Z_D| \leq 22$) relative to that seen for polymeric DNA. We propose a trapezoidal (for long oligomers) or a parabolic (for short oligos) axial counterion concentration model incorporating the CEE, and that oligolysine–DNA interactions are driven predominantly by salt ion release upon complex formation. Experimental data are qualitatively consistent with this model of ion accumulation along an oligomer. In particular, both $\log K_{obs}$ at fixed salt concentration and $|S_a K_{obs}|$ increase strongly with increasing $|Z_D|$ for DNA oligomers with no more than $|Z_L| + 2N_e$ phosphates, where N_e is estimated to be $\geq 11 \pm 4$ phosphates at 0.1 M and $\geq 7 \pm 3$ phosphates at 0.2 M salt. When $|Z_D| \geq |Z_L| + 2N_e$, the interior sites of the nucleic acid exhibit polymeric levels of ion accumulation, and binding becomes increasingly less sensitive to $|Z_D|$. Similarly, when multiple ligands (L^{8+}) bind to an intermediate-length DNA lattice at low to moderate salt concentrations, a CEE introduced by the first binding event weakens the affinity of the second binding event, consistent with a decrease in the extent of ion accumulation around the DNA complex with the first ligand. Quantitative analysis of short oligomer data and a more precise determination of N_e will be presented in a subsequent paper.

We demonstrate that binding depends strongly on the nucleic acid charge for short sequences and that the behavior of these systems is markedly different from that involving long polynucleotides. As a consequence, binding studies with highly charged ligands that use short nucleic acid oligomers as models of interior regions of polymeric RNA or DNA may exhibit quite different SK_{obs} and therefore different K_{obs} at low to moderate [salt]. Binding to ends of polyanionic or oligoanionic RNA or DNA will also exhibit different SK_{obs} (and K_{obs} at low [salt]) from interior binding. Characterization of CEEs in oligocation binding provides the information needed to compare end and interior binding.

SUPPLEMENTARY MATERIAL

Supplementary Material is available at NAR Online.

ACKNOWLEDGEMENTS

We would like to thank Prof. Timothy M. Lohman for generously providing all of the oligonucleotides used in this study, Chanokporn Sukopan for her technical assistance in the synthesis of KWK_6 and Michael W. Capp for his assistance with the peptide HPLC purification protocol. This research was supported by the University of Wisconsin-Madison.

REFERENCES

1. Olmsted,M.C., Anderson,C.F. and Record,M.T.,Jr (1991) Importance of oligoelectrolyte end effects for the thermodynamics of conformational transitions of nucleic acid oligomers: a grand canonical Monte Carlo analysis. *Biopolymers*, **31**, 1593–1604.
2. Shkel,I.A. and Record,M.T.,Jr (2004) Effect of the number of nucleic acid oligomer charges on the salt dependence of stability (ΔG^o_{37}) and melting temperature (T_m): NLPB analysis of experimental data. *Biochemistry*, **43**, 7091–7101.
3. Herschlag,D. (1991) Implications of ribozyme kinetics for targeting the cleavage of specific RNA molecules *in vivo*—more is not always better. *Proc. Natl Acad. Sci. USA*, **88**, 6921–6925.
4. Elbashir,S.M. (2001) Duplexes of 21-nucleotide RNAs mediate RNA interference in mammalian cell culture. *Nature*, **411**, 494–498.
5. Draper,D.E. (1995) Protein–RNA interactions. *Ann. Rev. Biochem.*, **64**, 593–620.
6. Perez-Canadillas,J.M. and Varani,G. (2001) Recent advances in RNA-protein recognition. *Curr. Opin. Struct. Biol.*, **11**, 53–58.
7. Hall,K.B. (2002) RNA–protein interactions. *Curr. Opin. Struct. Biol.*, **12**, 283–288.
8. Classen,S., Lyons,D., Cech,T.R. and Schultz,S.C. (2003) Sequence-specific and 3-end selective single-strand DNA binding by the *Oxytricha nova* telomere end binding protein R subunit. *Biochemistry*, **42**, 9269–9277.
9. Pilch,D.S., Kaul,M., Barbieri,C.M. and Kerrigan,J.E. (2003) Thermodynamics of aminoglycoside-rRNA recognition. *Biopolymers*, **70**, 58–79.
10. Stein,V.M., Bond,J.P., Capp,M.W., Anderson,C.F. and Record,M.T.,Jr (1995) Importance of Coulombic end effects on cation accumulation near

oligoelectrolyte B-DNA: a demonstration using ^{23}Na NMR. *Biophys. J.*, **68**, 1063–1072.
11. Anderson,C.F. and Record,M.T.,Jr (1995) Salt–nucleic acid interactions. *Ann. Rev. Phys. Chem.*, **46**, 657–700.
12. Record,M.T.,Jr, Zhang,W. and Anderson,C.F. (1998) Analysis of effects of salts and uncharged solutes on protein and nucleic acid equilibria and processes: a practical guide to recognizing and interpreting polyelectrolyte effects, Hofmeister effects, and osmotic effects of salts. *Adv. Prot. Chem.*, **51**, 281–353.
13. Latt,S.A. and Sober,H.A. (1967) Protein–nucleic acid interactions. III. Cation effect on binding strength and specificity. *Biochemistry*, **6**, 3307–3314.
14. Lohman,T.M., deHaseth,P.L. and Record,M.T.,Jr (1980) Pentalysine–deoxyribonucleic acid interactions: a model for the general effects of ion concentrations on the interactions of proteins with nucleic acids. *Biochemistry*, **19**, 3522–3530.
15. Mascotti,D.P. and Lohman,T.M. (1990) Thermodynamic extent of counterion release upon binding oligolysines to single-stranded nucleic acids. *Proc. Natl Acad. Sci. USA*, **87**, 3142–3146.
16. Mascotti,D.P. and Lohman,T.M. (1992) Thermodynamics of single-stranded RNA binding to oligolysines containing tryptophan. *Biochemistry*, **31**, 8932–8946.
17. Mascotti,D.P. and Lohman,T.M. (1993) Thermodynamics of single-stranded RNA and DNA interactions with oligolysines containing tryptophan. Effects of base composition. *Biochemistry*, **32**, 10568–10579.
18. Mascotti,D.P. and Lohman,T.M. (1997) Thermodynamics of oligoarginines binding to RNA and DNA. *Biochemistry*, **36**, 7272–7279.
19. Braunlin,W., Strick,T. and Record,M.T.,Jr (1982) Equilibrium dialysis studies of polyamine binding to DNA. *Biopolymers*, **21**, 1301–1314.
20. Plum,G.E. and Bloomfield,V.A. (1988) Equilibrium dialysis study of binding of hexammine cobalt (III) to DNA. *Biopolymers*, **27**, 1045–1051.
21. Record,M.T.,Jr, Lohman,T.M. and deHaseth,P. (1976) Ion effects on ligand–nucleic acid interactions. *J. Mol. Biol.*, **107**, 145–158.
22. Zhang,W., Bond,J.P., Anderson,C.F., Lohman,T.M. and Record,M.T.,Jr (1996) Large electrostatic differences in the binding thermodynamics of a cationic peptide to oligomeric and polymeric DNA. *Proc. Natl Acad. Sci. USA*, **93**, 2511–2516.
23. Zhang,W., Ni,H., Capp,M.W., Anderson,C.F., Lohman,T.M. and Record,M.T.,Jr (1999) The importance of Coulombic end effects: experimental characterization of the effects of oligonucleotide flanking charges on the strength and salt dependence of oligocation (L^{8+}) binding to single-stranded DNA oligomers. *Biophys. J.*, **76**, 1008–1017.
24. Bloomfield,V.A., Crothers,D.M. and Tinoco,I.,Jr (2000) *Nucleic Acids, Structure, Properties, and Functions*. University Science Books, Sausalito, CA.
25. Edelhoch,H. (1967) Spectroscopic determination of tryptophan and tyrosine in proteins. *Biochemistry*, **6**, 1948–1954.
26. Ferrari,M.E., Bujalowski,W. and Lohman,T.M. (1994) Co-operative binding of *Escherichia coli* SSB tetramers to single-stranded DNA in the $(SSB)_{35}$ binding mode. *J. Mol. Biol.*, **236**, 106–123.
27. Ferrari,M.E. and Lohman,T.M. (1994) Apparent heat capacity change accompanying a nonspecific protein–DNA, interaction. *Escherichia coli* SSB tetramer binding to oligodeoxyadenylates. *Biochemistry*, **33**, 12896–12910.
28. Fasman,G.D. (1976) *Handbook of Biochemistry and Molecular Biology: Nucleic Acids, 3rd edn*. CRC Press, Boca Raton, FL, Vol. 1, p. 589.
29. Lohman,T.M. and Mascotti,D.P. (1992) Nonspecific ligand–DNA equilibrium binding parameters determined by fluorescence methods. *Methods Enzymol.*, **212**, 424–458.
30. Epstein,I.R. (1978) Cooperative and non-cooperative binding of large ligands to a finite one-dimensional lattice. A model for ligand–oligonucleotide interactions. *Biophys. Chem.*, **8**, 327–339.
31. Johnson,M.L. and Fraiser,S.G. (1985) Nonlinear least-squares analysis. *Methods Enzymol.*, **117**, 301–342.
32. Anderson,C.F. and Record,M.T.,Jr (1993) Salt dependence of oligoion-polyion binding: a thermodynamic description based on preferential interaction coefficients. *J. Phys. Chem.*, **97**, 7116–7126.
33. Olmsted,M.C., Bond,J.P., Anderson,C.F. and Record,M.T.,Jr (1995) Grand canonical Monte Carlo molecular and thermodynamic predictions of ion effects on binding of an oligocation (L^{8+}) to the center of DNA oligomers. *Biophys. J.*, **68**, 634–647.
34. Record,M.T.,Jr and Lohman,T.M. (1978) A semiempirical extension of polyelectrolyte theory to the treatment of oligoelectrolytes: application to oligonucleotide helix–coil transitions. *Biopolymers*, **17**, 159–166.
35. Allison,S.A. (1994) End effects in electrostatic potentials of cylinders—models for DNA fragments. *J. Phys. Chem.*, **98**, 12091–12096.
36. Olmsted,M.C., Anderson,C.F. and Record,M.T.,Jr (1989) Monte Carlo description of oligelectrolyte properties of DNA oligomers: range of the end effect and the approach of molecular and thermodynamic properties to the polyelectrolyte limits. *Proc. Natl Acad. Sci. USA*, **86**, 7766–7770.
37. McGhee,J.D. and vonHippel,P.H. (1974) Theoretical aspects of DNA–protein interactions: co-operative and non-co-operative binding of large ligands to a one dimensional homogeneous lattice. *J. Mol. Biol.*, **86**, 469–489.
38. Bevington,P.R. and Robinson,D.K. (1992) *Data Reduction and Error Analysis for the Physical Sciences, 2nd edn*. McGraw Hill, Inc., New York, pp. 208–209.